Outflow-Infall Interactions Terminating Accretion in Protostellar Disks

T. Velusamy and W. D. Langer

MS 169-506, Jet Propulsion Laboratory, California Institute of Technology,

Pasadena, CA 91 109, USA

We present the first evidence for the process of terminating accretion in protostellar disks through the interaction between infall and a very wide opening angle outflow. The accretion phase in protostars is an important stage in planetary disk formation[1]. Langer, Velusamy & Xie[2] have shown that the Young Stellar Object (YSO) IRS1 in the dark cloud core Barnard 5 is the best example of a protostar with a wide opening angle outflow and is an ideal object for studying the effects of outflow-infall interactions. IRS1 is a relatively young object with a dynamical age of 10^4 yr for its molecular outflow[3] and PC scale optical jet[4]. Yet our data shows it to be in an advanced stage of disk accretion as indicated by wide opening angle outflow and narrow equatorial infall. It represents an important stage, late in the protostellar accretion phase, where flattened infall ancl wide angle outflow exist simultaneously. Our new interferometer data obtained with 1" resolution show that the outflow cones are widest at the vertices indicating a significant widening of the outflow with time. We suggest that this widening of outflow marks the final stages of isolating the disk from further accretion. We present a model to explain the shape and dynamics of the outflow and infall in terms of a coupling between the outflow and accretion near the star. We estimate that after the onset of outflow the entire accretion phase in IRS1 lasts only 20,000 yr.

Shortly after the onset of protostellar collapse, the inner regions of t he collapsing core form a protostar and nebular disk[5]. The infalling envelope of gas and dust leads to further growth of this disk and p rot ost ar. This accretion phase i s estimated to last about 10^5

years. Sometime during this accretion phase a bipolar outflow develops along the rotation axis, consisting of a narrow high velocity jet and a lower velocity but spatially broader molecular outflow'. The force of this molecular wind is sufficient to reverse the infall and sweep out material along the poles within the bipolar outflow cones. We show that in time the outflow greatly modifies the infall geometry changing it from a spherical to an equatorial accretion region. Eventually the point is reached where it shuts off' the infall completely. Subsequently the disk enters the planet formation stage. The stage when infall and outflow exist simultaneously is a very important but little understood phase of protostar and disk evolution. It may control the final mass of both the protostar and protoplanetary disk.

Only recently has data become available close to the star, in a couple of objects. on the molecular outflow and infall[2,6-10]. Yet none of these observations have focused on the out flow-infall interaction] and the subsequent effects on the disk evolution. Here we report new interferometric images which resolve the velocity fields in the infall and outflow closest to the protostar IRS1 in B5, a Class I object with luminosity $\sim 9.6\ L_{\odot}$ located at a distance of 350 pc. We obtained CO(2-1) isotope maps, of the disk, infall, and outflow with Caltech's Owens Valley Radio observatory Millimeter Array (OVRO-MMA). The observations were made in 1996-97 using the six-element array in both the high and low resolution configurations to obtain the best u-v coverage and the highest resolution available, $\sim$ 1" at 1.3 mm. The $C^{18}O$(2-1) traces the dense infalling gas, while the line wings of ^{12}CO(2-1) trace the molecular outflow.

The OVRO maps illustrate the first direct evidence of very wide angle molecular outflow cones close to the star (< 1000 AU) accompanied by equatorial infall. Figure 1 shows our high resolution (1" to 2") maps of the 1.3 mm continuum, ^{12}CO(2-1) and $C^{18}O$(2-1). The most remarkable feature revealed in these maps is the geometrical shapes and clear demarkation of the outflow and infall boundaries. The $C^{18}O$(2-1) emission shows that the infall is confined to a narrow equatorial region perpendicular to the jet's outflow axis, while ^{12}CO(2-1) maps show that the high velocity outflow originates in bipolar cones which can be traced deep down to within 0.1" (150 AU) from the star. The continuum disk at 1.3 mm is compact 1.2" x 1.0" (420.1" x 350 AU) and contains $\sim$ 0.02 $M_{\odot}$ of gas and dust as determined from the

dust emission assuming a standard gas to dust ratio of 100. The star's position inferred from the continuum disk is $\sim$ 1.2.5" away from the IRAS infrared position[11], and has an accuracy better than 0.1" and, therefore, we adopt this for the star's position.

Equatorial infall: Figure 2a shows selected $C^{18}O$(2-1) velocity channel maps. The velocity field as indicated in these maps is dominated by infall motions rather than rotation. The channel map at the rest velocity (center panel, $\Delta V = V - V_{lsr} = 0$ km s^{-1}) traces the infalling gas which has a zero velocity component along the line of sight with respect to the systemic LSR velocity of IRS] ($V_{lsr} = 10.2$ km s^{-1}). In other words this channel map shows the full intent of the infall occurring in the plane of the sky. As seen in this panel the butterfly shape and extent of the infall region is consistent with an initially spherical infall which has been modified by the large opening angle outflow.

The other velocity channel maps represent the infall gas located out of the plane of the sky ($\Delta V < 0$ on the fat side, and $\Delta V > 0$ infalling gas on the near side). The highest velocity channel maps (left and right panels) will snow the gas which has the largest infall velocity component along the line of sight. Since the infall velocity increases towards the center (higher density $\Rightarrow$ larger sound speed) the gas in the immediate vicinity of the protostar will show the largest infall velocities. Therefore, maps at ($\Delta V = \pm$ 0.9 km s^{-1}) will have the most compact emission centered near the star. The overall emission pattern in the $C^{18}O$(2-1) velocity maps is consistent with radial infall motions directed towards the star. within a flared disk, $\sim$ 10" x 5" (3500 x 1800 AU) which is inclined at $\sim 45°$ to the plane of sky, and contains a mass of $\sim$ 0.08 $M_\odot$ (assuming no depletion and $\frac{N(H_2)}{N(C^{18}O)} = 5 \times 10^6$). The infall region is strictly confined to the equatorial zone and avoids the outflow (Fig. 1). Within the infall region there is an indication of a small rotational velocity gradient $\sim$0.1km s^{-1} (1000 AU)$^{-1}$ close to the star at r < 1000 AU.

Bipolar Outflow Cones: Recent observations show compact outflows with a biconical structure near their stars[2,12]. However, thin' observations did not resolve the detailed structure of the cones closest to the star. Figure 2b shows our channel maps of ^{12}CO(2-1) emission in the red and blue shifted outflow lobes with a spatial resolution of 1.2" x 1.0" at 2 km s-^{1} velocity spacing. Such high resolution brings out the geometrical shape of the outflow

lobes on very small scales ($\sim$ 100 AU) at distances from 100 AU to 10,000 AU. These interferometer images resolve out the flux at larger scales ($\geq$ 15" in the 1.3 mm OVRO maps). However this missing flux does not affect our conclusions concerning the geometrical shape of the outflow lobes (Figs. 1-3), especially the structures near the vertices (within a $\sim 5''$ radius) which are fully represented in the interferometer images. Even at larger distances the missing flux in the short spacings is not a limitation to defining the outflow boundary, because the interferometer acts only as a highpass spatial filter.

The outflow cones are seen best in the $\pm$ 3 km s^{-1} velocity emission (Fig. 2b), and in the integrated emission of the blue lobe (Fig. 3). Taken together our images show: (i) The CO outflow lobes exhibit bipolar conical structure, and their vertices lie symmetrically on either side of the star within 0.4" (150 AU). (ii) The limb brightened cones have a sharp outer boundary, a hollow interior indicating a void in molecular material, aud the cone walls are thin ($\sim$ 500 AU). (iii) Small scale structures ($\sim$ a few hundred AU in size) are seen in the outflow cones, which we suggest are evidence of episodic outflow activity. (iv) Over the extent of the interferometer map we do not see any evidence of 'Hubble flow' (i.e. the peak velocity increasing roughly with distance) as seen in single dish, large scale maps[12]. The mean outflow velocity is nearly constant (at 6 km s^{-1}) across the lobes, hence the structures seen within 1 000 AU are the result, of the outflow generated in the recent past, within 1000 yr. (v) The momentum distribution (proportional to the integrated intensity, which is a measure of mass, x the mean outflow velocity) along the outflow axis peaks at the origin of outflow and decreases outward. Our estimate of the momentum distribution near the star, where the structures are small, is accurate, but this becomes less reliable at larger distances because the interferometer maps do not image the large scale structures. Nevertheless, our data is sensitive enough to show a momentum peak at the origin of the outflow. While the current models[13-17] can explain some of these observed outflow properties none seem to explain all of them, especially the geometry of the outflow both at the origin and at larger distances.

Time evolution and widening of the outflow cones: The observational data indicate that outflow energetics decrease with evolutionary status of the YSO[18]. This decrease implies

a corresponding decrease in the mass accretion, if infall fuels the outflow. If this is true we expect to see an out flow-infall interaction. Here we pl('writ new evidence of such an int tract ion and discuss its effects on disk accret ion. In Figs. 1-3 the bipolar out flow is seen to have evacuated a biconical cavity whose limb brightened walls appear to be pushing and compressing the ambient and/or infalling gas.

The outflow lobe st ruct ure is best seen in t he blue shifted emission (Fig. 3). Wit hin t he blue lobe there is some asymmet ry in the CO(2-1) int ensity along the NE and SE direct ions, which is also observed in the i-band image of scatted light seen through t he evacuated out flow cavities[19], and in the CO(1-0) emission[2]. At the vertex the out flow appears to be quite symmetrical out to $\sim$ 1000 AU. The lobe boundary is well defined and continuous along the NE direction even to large distances, up to 10,000 AU. Therefore, we have chosen to use this part of the blue lobe to derive the time evolution of the geometry of the out flow. The geometrical shape of the outflow close to the star is bet ter described as parabolic t han conical. We interpret this parabolic shape in terms of an increase in the out flow cone angle with time due to the lateral expansion of the outflow at the vertex, in a direction perpendicular to the jet axis. In Fig. 3 we indicate the extent of the outflow in the cones at several epochs as in ferred from the shape of the bou ndary, and assuming a mean out flow velocity of ~ 6 km s^{-1} along the cone. The geometrical shape at t he vertex, which describes the out flow wit hin the past 1000 yr is consistent with an opening angle of $\sim 126°$, while at larger dist ances from the vertex it is narrower, for example at 6000 AU (representing the outflow originating about 6000 yr ago) the corresponding opening angle is $\sim$ 92°. This difference implies a widening of the opening angle $\sim$ 0.006° yr^{-1}.

The data presented here indicate that the widening oft he out flow cones and t he flat tening of the infall must be coupled to each other through the processes involved in generating the molecular outflow near the star. A qualitative interpretation is given here and a detailed model will be presented later. For simplicity we consider a jet-driven-t horough-shock model[15] for the outflow mechanism. In this model t he average momentum is directed nearly parallel to t he out flow axis, with a small t ransverse component. The outflow properties will depend on the nat ure of t he momentum t ransfer to the molecular flow. The momentum transferred by

t he jet to the outflow per unit le ngt h along the out flow axis is related to the ambient density ρ_a and is given by[20] $P_z \sim \pi r_j^2 v_j \sqrt{\rho_a \rho_j}$, where ρ_j, r_j, v_j are t he density, radius, and velocity of the jet, respect ively. Therefore we expect t he geomet ry and intensity of t he out flow to depend on the location, extent, and shape of t he region of momentum t ransfer, which in t urn is determined by the density distribution in the disk and envelope. We conclude from our data that the largest momentum transfer is occurring closest to the star (< a few hundred AU) as predicted by both wind and jet/sllock driven out flows[16,20]. This result is consistent with the region of the highest density being most effective in transferring momentum. However, the density structure at this outflow-disk interface is continuously modified by a balance between the evacuation) by outflow and the accretion from infall.

The time evolution of the outflow-infall interaction can be summarized by a simple feedback mechanism. At the initiation of the jet the infall is spherical, the density distribution is broad and the outflow is narrow angled. As the outflow proceeds material is swept out of the outflow cones, simultaneously reducing the accretion volume, by narrowing the extent over which infall occurs (Fig. 1). This interaction sets up a negative feedback in that the increase in the opening angle of the outflow cones, creates a wider evacuated cavity above the disk-jet interface and further narrows equatorial infall. We speculat e that the resultant density st ruct ure at the origin of the out flow leads to the momentum t ransfer occurring in a wider angle, thus forming a still larger opening angle out flow. This process continues until the outflow opening angle approaches 180° and the infall is shut down completely. thus terminating disk accretion.

In summary, we show the clearest evidence yet of an out flow-infall int tract ion. leading to an equatorial infall, and providing a natural mechanism for the end of infall, and hence, the end of the accreting phase in YSOs. We find evidence for the widening of the opening angle of tile outflow cones. By tracing the time evolution in the out flow cones, we estimate that the infall will be totally shut down in $\sim 10^4$ yr in IRS1 in B5. Therefore, once out flow begins, typically the entire accretion phase lasts only $\sim$ 20,000" yr.

References

[1] Beckwith, S. & Sargent, A. I. *Circumstellar disks and the search for neighbouring planetary systems, Nature* 383, 139-144 (1996).

[2] Langer, W. D., Velusamy, T. & Xie, T. *IRS 1 circumstellar disk and the origin of the jet and CO outflow in B5, Astrophys. J. Lett.* 486, 1.41-1,44 (1996).

[3] Goldsmith, P.F., Langer, W.D. & Wilson, R. W. *Molecular outflows, gas density distribution, and the effects of star formation in the dark cloud Barnard 5, Astrophys. J. Lett.* 303, 1,11-1,15 (1986).

[4] Bally, J., Devine, D. & Alten, V. *A parsec-scale Herbig-Haro jet in Barnard 5, Astrophys. J.* 473, 921-928 (1966).

[5] Shu, F., Najita, J., Galli, D., Ostriker, E. & Lizano, S. in *Protostars and Planets III* (eds. E.H. Levy aud J.I. Lunine) 3-45 (The Univ. of Arizona Press: Tucson, 1993)

[6] Chandler, C., Terebey, S., Barsony, M., Moore, 'I'. J."J'. & Gautier, T.N. *Compact outflows associated with TMC-1 and TMC-1A, Astrophys. J.* 471, 308-320 (1966).

[7] Chandler, C. & Sargent, A.I. *The small scale structure and kinematics of B335, Astrophys. J. Lett. 486,* 1,29-1.32 (1993).

[8] Velusamy, T., Kuiper, T.B.H. & Langer, W.D. *Imaging infall: CCS observations of protostellar* envelope of *B335, Astrophys. J. Lett.* 451, 1,75-1,78 (1995).

[9] Bachiller, R., Guilloteau, S. & Dutrey, A. *Jet driven molecular outflow in 1,1118-C. CO and continuum synthesis images, Astron. A strophys.* 299, 857-868 (199.5).

[10] Gueth, F., Guilloteau, S., Dutrey, A. & Bachiller, R. *Structure and kinematics of protostar: mm-interferometry of L1157, Astron. Astrophys. 323, 943-952* (1997).

[11] Beichman, C.A., et al. *Formation of solar type stii'c$: IRAS observations Of the dark cloud Barnard 5, Astrophys. J. Lett.* 278, 1,45-1,48 (1981).

[12] Ladd, C.J. & Fich, M. *The structure and energetics of a highly collimated bipolar* outflow: *NGC 2264 G, Astrophys.,1.459,* 638--652 (1996).

[13] Stabler, S. *The kinematics of molecular outflows, Astrophys. J. 422, 616-620 (199.1).*

[14] Raga, A.C., Cantó, J., Calvert, N., Rodriguez, L.F. & Torrelles, J. M. *A unified stellar jet/molecular outflow model, Astron. Astrophys.* 276, 539-5482 (1993).

[15] Masson, C.R. & Chernin, L.M. *Properties of jet-drillc?l molecular outflows, Astrophys. J.* 414, 230-241 (1993).

[16] Ii, Z.-Y & Shu, F.H. *Magnetized singular isothermal toroids, Astrophys. J.* 472,211-224 (1996).

[17] Smith, M.D., Suttner, G. & Yorke, H.W. *Numerical hydrodynamical simulations of jet-driven bipolar outflows, Astron. Astrophys.* 323, 223-230 (1997).

[18] Bontemps, S., Andre, P., Terebey, S. & Cabrit, S. *Evolution of outflow activity around low-mass embedded young stellar objects, A stron. Astrophys. 311,* 858-872 (1996).

[19] Heyer, M.H., Ladd, E1'., Myers, P.C. & Campbell, B. *Infrared and optical imaging of newborn stars, Astron. J.* 99, 1585-1597 (IWO).

[20] Chernin, L.M. & Masson, C. R. *Momentum distribution in* **molecular** *outflows, Astrophys. J. 455, 182-189* (1995).

We thank the Caltech's OVRO staff for their assistance and support. The Owens Valley Radio observatory millimeter-wave array is supported by the NSF. This research was conducted at the Jet Propulsion Laboratory, California Institute of Technology, under contract with the National Aeronautics and Space Administration.

Correspondence should be addressed to T.V. (e-mail: velu@rams.jpl.nasa.gov)

Figure 1: An overview of the infall-outflow interaction in IRS1 in B5. (a) Integrated I²['()(2-1) emission tracing the molecular outflow cones. The red and blue arrows denote red and blue shifted lobes, while the short black arrows denote the widening of the outflow cones. The values of the first contours and contour intervals are 0.45 & 0.'3 Jy km s⁻1 (beam)⁻¹ for the blue lobe, and 1.2 & 2.4 Jy km s⁻1 (beam)⁻¹ for the red lobe, respectively. (b) $C^{18}O$(2-1) emission tracing the infall region. The extent of the equatorial infall is a flared disk $\sim 30°$ wide as indicated in the Figure. The diameter of the disk is $\sim$3500 AU (10"), and the thickness varies from 850 AU at the center to 1700 AU at the edge. The values of the first contour and contour interval are 0.24 Jy km s^{-1} (beam)$^{-1}$. The inset in (b) shows the 1.3 mm continuum emission, whose first contour and contour interval are 5 mJy (beatn)'1. In Figs. 1-3 the offset position (0,0) corresponds to the IRAS position, the crosses represent the continuum peak at RA(1950): 03"44"'31 .^{s}98 $\pm$0.^{s}009; Dec(1950): 32 °42'31 ."24 $\pm$0."06, and the solid ellipses in the bottom left corner denote the size of the beams.

Figure 2: Selected channel maps of infall and outflow, with the velocities indicated in each panel. (a) The structure of $C^{18}O$(2-1) emission as a function of velocity indicates radial infall motions within a flared disk. The first contour is 0.8 Jy (beam)⁻¹ and contour interval is 0.2 Jy (beam)⁻¹. The SE-NW line through the center represents the equatorial plane which is inclined at 45° to the plane of sky. (b) ^{12}CO(2-1) velocity structure of red and blue shifted outflow lobes. The first contour and contour interval are 0.15 Jy (beam)" ¹ for the blue and, 0.2 Jy (beam) - ¹ for the red lobes.

Figure 3: Time evolution of the outflow cones is shown 011 the integrated intensity map of the blueshifted out flow lobe. The direction of the jet inferred from the optical data at pc scales is indicated. The intensities are in Jy km s^{-1} (beam)$^{-1}$. The first contour is 0.24, and contour intervals are 0.24 for the first 6 contours and ().-18 for the rest. The extent of the out flow cones and direction of gas flow at the epochs shown are derived assuming a mean outflow velocity of 6 km s⁻ ' .

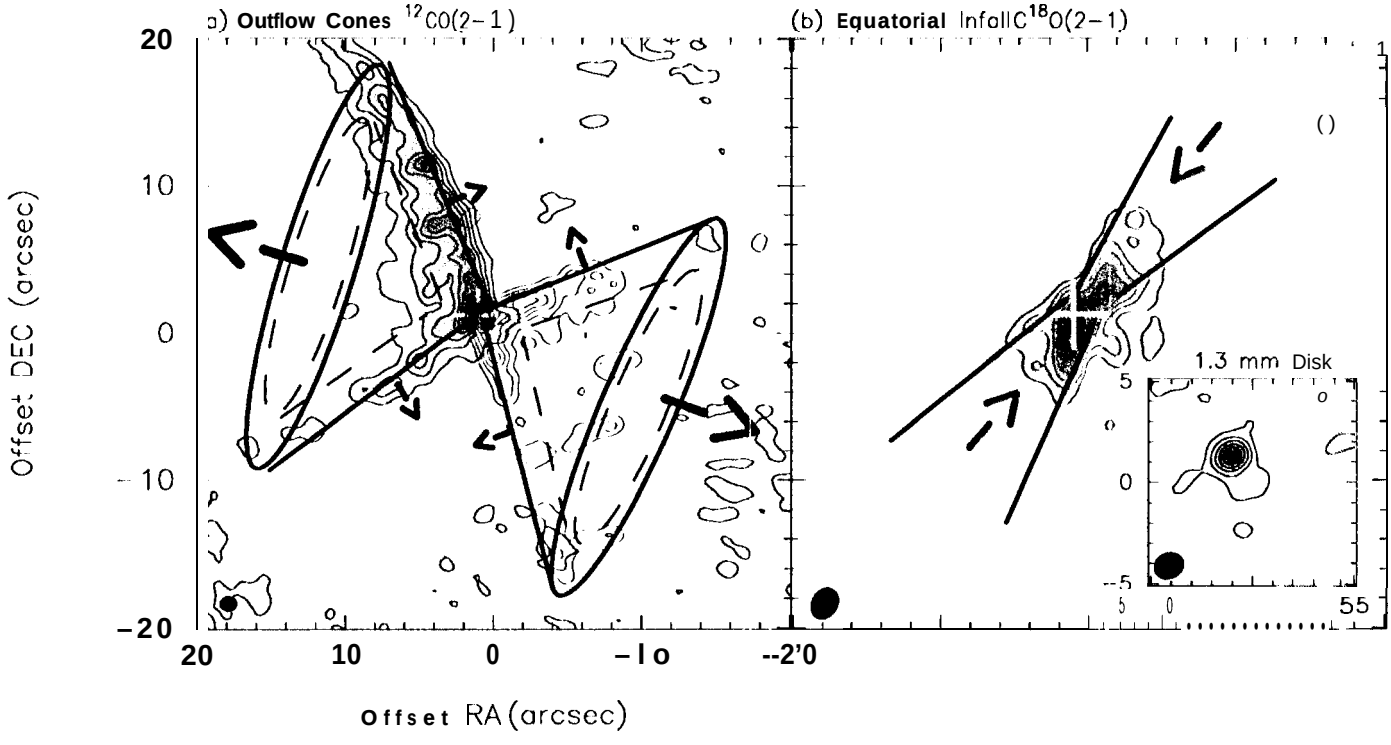
a) Outflow Cones $^{12}CO(2-1)$
(b) Equatorial Infall $C^{18}O(2-1)$
1.3 mm Disk
Offset DEC (arcsec)
Offset RA (arcsec)
20
10
0
-10
-20
20
10
0
-10
-20

Fig. 1

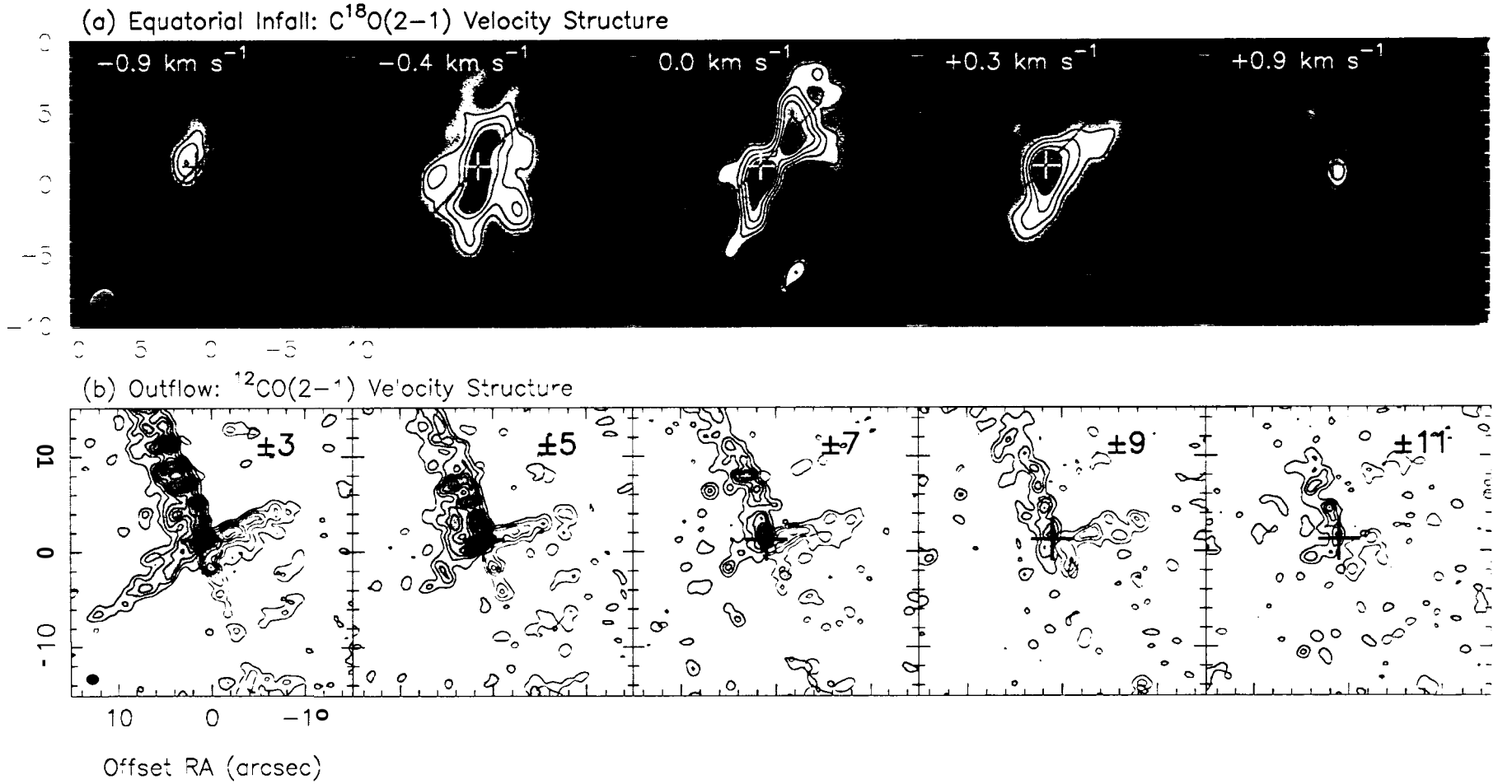
(a) Equatorial Infall: $C^{18}O(2-1)$ Velocity Structure
−0.9 km s^{-1}
−0.4 km s^{-1}
0.0 km s^{-1}
+0.3 km s^{-1}
+0.9 km s^{-1}
(b) Outflow: $^{12}CO(2-1)$ Velocity Structure
±3
±5
±7
±9
±11
Offset DEC (arcsec)
Offset RA (arcsec)

Fig. 2

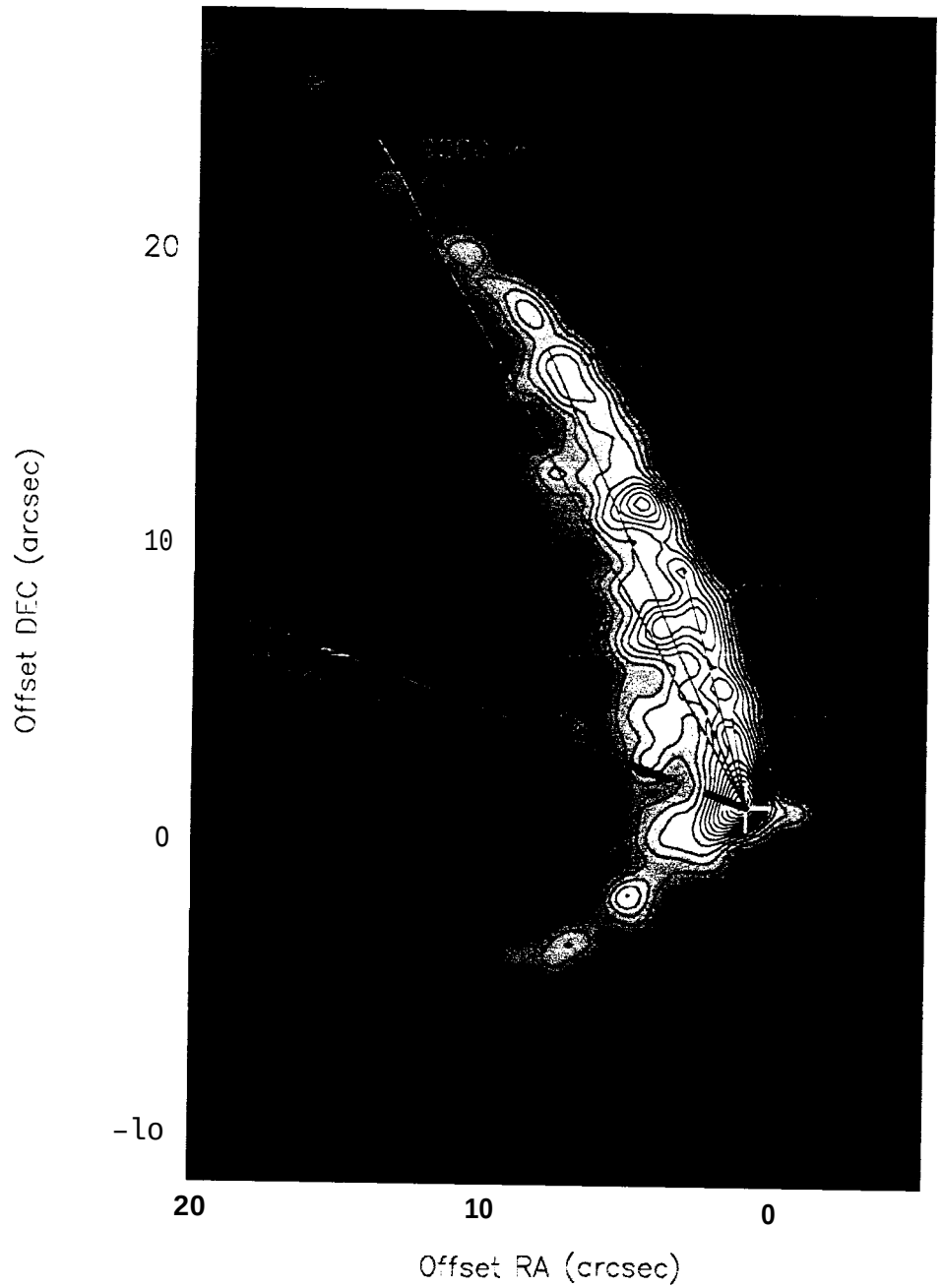

Fig. 3